JOURNAL OF GUIDANCE, CONTROL, AND DYNAMICS
Vol. 20, No. 6, November–December 1997

Simultaneous Structural/Control Optimum Design of Composite Plate with Piezoelectric Actuators

Youdan Kim* and Dongjun Kum†
Seoul National University, Seoul 151-742, Republic of Korea
and
Changho Nam‡
Hankuk Aviation University, Koyang 411-791, Republic of Korea

An integrated structural/control design for the vibration suppression of a composite plate with segmented piezoelectric (PZT) actuators is examined. The electric power used by the PZT materials becomes a very important factor for real application to the control of flexible structures. The method to predict power required for the control is presented, and the power is used as a part of the objective functions. The structural weight, the state error energy, control energy, stability robustness, and the electric power required for vibration control are considered as the objective function. The locations of the PZT actuators are considered as control design variables. The ply orientation and thickness coefficients of the laminated composite plate are considered as structural design variables. The improved compromise multiobjective optimization by using a reduction factor of performance indices is applied to solve this optimization problem. The sequential linear programming method with move limits is used. The sensitivity analysis, which is required in the optimization process, is performed for the eigenstructure assignment control scheme and the performance indices with respect to the design parameters. The optimized results showed a significant amount of reduction in the structural weight as well as the control performance indices. The required electric power is also decreased.

I. Introduction

LARGE flexible space structures have very low natural frequencies and damping and, therefore, an active control system is required. The designs of the structure and the control systems are usually carried out separately. The structure has been optimized from a stiffness point of view to raise modal frequencies as high as possible within weight and load constraints, whereas the actuator locations have been selected to minimize the control energy. With the recent increase in demand for structures having integrated control systems, interaction between the structure and the control system becomes an essential factor and plays an important role in the design. Because of the interaction between the control system and the structure system, the simultaneous design for a flexible structure via an optimization method has received much attention.[1–8] Rao et al.[9] provided a method of vibration control of flexible space structures by simultaneously integrating structure design and control system design.

A recent application of piezoelectric (PZT) materials for structural vibration suppression has added new dimensions to the control system. Because of the direct and converse effects of PZT materials, the dream of an intelligent structure, which is defined as a structure with the integrated sensor/actuator system, is beginning to be realized. Analytic and experimental studies for an induced strain actuator coupled with beams and plates have been developed by many authors.[10–15] Hanagud et al.[16] developed the optimal control algorithm that is applicable to flexible beam structures with PZT sensors and actuators. The power prediction becomes an important issue in the application of the PZT materials. Several papers that addressed the prediction of power consumption have been presented.[17,18] Our previous study has been extended in this paper.[19] The objective is to present a new approach for an integrated optimum design of the structure and control system, considering competing structural/control design objectives. The segmented PZT actuators are used for vibration control of the laminated composite plate. The analysis of the laminated composite wing with segmented piezoelectric actuators is conducted by the Rayleigh–Ritz method. To design the control system, a robust eigenstructure assignment scheme is adopted.

Five structural/control cost functions, the structural weight, the state error energy, control energy, stability robustness, and the electric power required for the control, are minimized over design variables, which include structural as well as control parameters. The locations of the PZT actuators are considered as control design variables. The ply orientation and the thickness coefficients of the composite layers are considered as structural design variables. The integrated structure/control design is formulated as a constrained multiobjective optimization problem. For most structure/control interaction problems, a tradeoff between structural objective and control objective is needed. The improved compromise multiobjective optimization by using a reduction factor of five design objectives is applied to solve the optimization problem. Constraints are imposed on the natural frequency, tip displacement, and twist due to point loads. To solve the optimization problem, the sequential linear programming method is utilized.

II. Modeling of Adaptive Structures

The laminated plate with eight PZT actuators, which are attached on the surface (as shown in Fig. 1), is taken as a model to be designed. Forces and moments acting on the laminated composite plate with segmented PZT actuators are derived by the classical laminate plate theory. In-plane forces and moments of the laminated plate including the loads of the PZT actuators are obtained by integrating stresses over the ply thickness and, thus, are expressed as follows[2,7]:

$$\{N\} = \int \{\sigma\}\,\mathrm{d}z = [A_s]\{\epsilon\} + [B_s]\{\kappa\} - \{N_\Lambda\} \tag{1}$$

$$\{M\} = \int \{\sigma\} z\,\mathrm{d}z = [B_s]\{\epsilon\} + [D_s]\{\kappa\} - \{M_\Lambda\} \tag{2}$$

where $\{\epsilon\}$ and $\{\kappa\}$ are the midplane strain and curvature; and $[A_s]$, $[D_s]$, and $[B_s]$ are extension, bending, and extension/bending

Received Nov. 18, 1996; presented as Paper 97-0246 at the AIAA 35th Aerospace Sciences Meeting, Reno, NV, Jan. 6–9, 1997; revision received July 30, 1997; accepted for publication July 31, 1997.

*Associate Professor, Department of Aerospace Engineering. E-mail: ydkim@plaza.snu.ac.kr. Senior Member AIAA.
†Graduate Student, Department of Aerospace Engineering.
‡Assistant Professor, Department of Aeronautical and Mechanical Engineering. Senior Member AIAA.

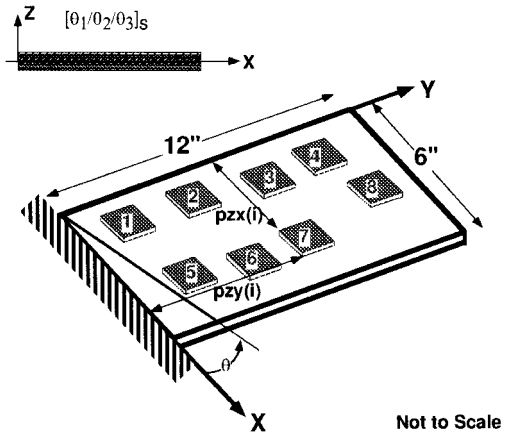

Fig. 1 Laminated plate model with PZT actuators.

coupling stiffness matrices, respectively. These matrices are influenced by the geometry of the piezoactuators. $\{N_\Lambda\}$ and $\{M_\Lambda\}$ are in-plane forces and moments due to actuator strain, respectively.

The Rayleigh–Ritz method involves assumption of the displacement functions such that they satisfy the boundary conditions. For the control system design of a symmetric laminated plate model with PZT actuators, the model is assumed to have the surface bonded piezoelectric actuators on the opposite side of the plate at the same location. It is also assumed that the same magnitude but the opposite direction of electric field is applied to the actuator so as to create a pure bending moment for vibration suppression. With these assumptions, the in-plane strains can be neglected. To approximate the out-of-plane displacement on the model, we used the free-free beam vibration modes in the x direction and the cantilever beam vibration modes in the y direction.

Using these displacement functions, the strain energy and kinetic energy can be written in generalized coordinates as[17,20]

$$U = \tfrac{1}{2}\{q\}^T[K_s]\{q\} - \lfloor Q_\Lambda \rfloor\{q\} \tag{3}$$

$$T = \tfrac{1}{2}\{\dot{q}\}^T[M_s]\{\dot{q}\} \tag{4}$$

Applying Lagrange's equation results in a set of ordinary differential equations of motion. After the modal analysis, a model reduction is performed using the first n_r lowest vibration modes to obtain a set of equations of motion in modal coordinates,

$$[\bar{M}_s]\{\ddot{\bar{q}}\} + [\bar{K}_s]\{\bar{q}\} = [\bar{F}_p]\{u\} \tag{5}$$

where $[\bar{M}_s]$ and $[\bar{K}_s]$ are the generalized mass and stiffness matrices including the effect of the piezoelectric actuators placement and $[\bar{F}_p]$ is the control force matrix due to unit electric voltage. Introducing the state vector $\{x\}^T = \lfloor \bar{q} \;\; \dot{\bar{q}} \rfloor$, Eq. (5) can be written as the following state equation:

$$\{\dot{x}\} = [A]\{x\} + [B]\{u\} \tag{6}$$

where

$$[A] = \begin{bmatrix} [0] & [I] \\ -[\bar{M}_s]^{-1}[\bar{K}_s] & [0] \end{bmatrix}, \qquad [B] = \begin{bmatrix} [0] \\ [\bar{M}_s]^{-1}[\bar{F}_p] \end{bmatrix}$$

and state vector $\{x\} \in R^n$, control vector $\{u\} \in R^m$, $n = 2 \times n_r$, and m is the number of PZT actuators. In this study, the first 10 vibration modes are used to obtain the reduced order model.

III. Control System Design

The eigenstructure assignment regulator (EAR) theory is employed to suppress the vibration with the smallest control effort. It is assumed that all states are available for feedback. Consider the completely controllable and observable linear dynamic system in the state-space form

$$\{\dot{x}\} = [A]\{x\} + [B]\{u\} \tag{7}$$

with the linear feedback control

$$\{u\} = -[G]\{x\} \tag{8}$$

The right and left eigenvalue problems of the closed-loop system can be written as

$$\begin{aligned} ([A] - [B][G])\{\phi^c\}_i &= \lambda_i^c\{\phi^c\}_i \\ ([A] - [B][G])^T\{\psi^c\}_i &= \lambda_i^c\{\psi^c\}_i \end{aligned} \tag{9}$$

where $\{\phi^c\}_i$ and $\{\psi^c\}_i$ are the right and left eigenvectors of the closed-loop system, respectively, corresponding to the eigenvalue λ_i^c. We adopt the conventional normalization of the biorthogonality conditions for the eigenvectors as

$$\{\phi^c\}_i^T\{\phi^c\}_i = 1, \qquad \{\psi^c\}_i^T\{\phi^c\}_i = 1 \tag{10}$$

where $(\,)^T$ denotes the transpose of the given vector.

The desired closed-loop eigenvalues are chosen by considering the open-loop eigenvalues λ_i^o as follows:

$$\lambda_i^c = -\frac{\Im(\lambda_i^o)\zeta_i}{\sqrt{1-\zeta_i^2}} + j\Im(\lambda_i^o) \tag{11}$$

where $\Im(\,)$ denotes the imaginary part of the given value. By taking the desired eigenvalues as Eq. (11), the damping ratio ζ_i is assigned to the ith mode of the closed-loop system, and the imaginary part that is related to the natural frequency is retained.

The pole placement algorithm based on Sylvester equation utilizes the parameter vector $\{h\}_i$ defined by[21]

$$\{h\}_i = [G]\{\phi^c\}_i \tag{12}$$

Substituting Eq. (12) into Eq. (9) yields the following Sylvester equation:

$$([A] - \lambda_i^c[I])\{\phi^c\}_i = [B]\{h\}_i \tag{13}$$

or, in matrix form,

$$[A][\Phi_c] - [\Phi_c][\Lambda_D] = [B][H] \tag{14}$$

where

$$\begin{aligned} [\Phi_c] &= \left[\{\phi^c\}_1, \{\phi^c\}_2, \ldots, \{\phi^c\}_n\right] \\ [\Lambda_D] &= \operatorname{diag}\begin{pmatrix} \lambda_1^c & \lambda_2^c & \cdots & \lambda_n^c \end{pmatrix} \\ [H] &= [\{h\}_1, \{h\}_2, \ldots, \{h\}_n] \end{aligned} \tag{15}$$

Note that $[\Lambda_D]$ contains the desired closed-loop eigenvalues.

The main steps of robust eigenstructure assignment algorithm for vibration control are summarized as follows.[22,23] First, select a target eigenvector $[\Phi_T]$. In vibration control problems, it is known that open-loop eigenvectors are well conditioned and a good choice of a family of admissible target vectors.[22] The open-loop eigenvectors are adopted as the target eigenvector. Second, compute $[H]$ matrix by solving the Sylvester equation in the least square sense,

$$[H] = [B]^\dagger([A][\Phi_T] - [\Phi_T][\Lambda_D]) \tag{16}$$

where $(\,)^\dagger$ is the pseudoinverse of the matrix $(\,)$. Now, solve the Sylvester equation (14) to obtain closed-loop eigenvector matrix $[\Phi_c]$ and, finally, compute the gain matrix using relation (12):

$$[G] = [H][\Phi_c]^{-1} \tag{17}$$

An equivalent real type Sylvester equation may be formulated.[23] With this formulation, more accurate results can be obtained with less numerical effort.

IV. Power Required for the Control

The electric power required for vibration control is defined and used as a part of the objective functions. The electric charge due to the direct effect of the PZT materials is[17]

$$Q_i = k_s \int_{A_{pi}} D_{3i}\,\mathrm{d}x\,\mathrm{d}y = k_s[\bar{F}_p]^T\{q\} + [D]\{u\} \equiv [C]\{x\} + [D]\{u\} \tag{18}$$

The electric current flowing through the PZT actuators is obtained by taking the time derivative of the electric charge stored due to the direct effect of the PZT materials.

When the voltage $\{u\}$ applied to the actuators and the measured current $\{I\}$ are given by

$$\{u\} = \{V_0\}\sin(\omega t) \tag{19}$$

$$\{I\} = \{I_0\}\sin(\omega t + \phi) \tag{20}$$

then the admittance matrix $[H]$ of the open-loop system is expressed in the following form[17,18]:

$$[H(i\omega)] = (j\omega/k_s)[[C][j\omega[I] - [A]]^{-1}[B] + [D]] \tag{21}$$

For the calculation of the electric current, it is assumed that the disturbance forces $\{u_r\}$ are exerted harmonically with a specified amplitude on the surface of the PZT actuator:

$$\{u_r\} = \{V_r\}\sin(\omega t) \tag{22}$$

The amplitude $\{V_r\}$, which is the signal obtained from the PZT actuators with a charge amplifier, is expressed as

$$\{V_r\} = k_s[\bar{F}_p]^T\{q_0\} = [C]\{x_0\} \tag{23}$$

Similarly, in the closed-loop system, if the voltage $\{V_r\}$ is exerted harmonically on the surface of the PZT actuators due to a disturbance, the current required for the control is expressed as[17]

$$\{I_0\} = (j\omega/k_s)\Big[[C_c](j\omega[I] - [A_c])^{-1}[B] + [D]\Big]\{V_r\} \tag{24}$$

where $[A_c] = [A] - [B][G]$ and $[C_c] = [C] - [D][G]$.

The amplitude of the harmonic motion $\{x_o\}$ is given arbitrarily. The electric power, which is the apparent power, is obtained from Eq. (24) by multiplying the applied control voltage.

V. Integrated Structure/Control Design

Using the equations presented in the preceding sections, the integrated optimal design is conducted for vibration suppression. For most structure/control interaction problems, a tradeoff between structural objectives and control objectives is needed. In this paper, the improved compromise multiobjective optimization is applied. In the improved compromise multiobjective optimization method, the objective function is expressed as follows[7]:

$$\mathcal{J}(\boldsymbol{p}) = \sqrt{\sum_{i=1}^{n_i} W_i^2 \left| \frac{r_f J_i(\boldsymbol{p})}{(J_i)_{\max} - (1 - r_f)J_i(\boldsymbol{p})} \right|^2} \tag{25}$$

where W_i is the weighting factor for the ith objective function J_i; r_f is the reduction factor; $(J_i)_{\max}$ is taken as the initial objective function value, which is evaluated by the given initial design variables; and n_i is the number of the objective functions.

The structural objective function J_1 is the weight of the composite plate and is expressed as follows[7]:

$$J_1 = \sum_{i=1}^{nop} \int_x \int_y \bar{\rho} t_i(x, y)\,\mathrm{d}x\,\mathrm{d}y \tag{26}$$

where $\bar{\rho}$ is density of the composite plate, $t_i(x, y)$ is the thickness distribution of the ith ply, and nop denotes the number of the composite layers.

State error energy, control energy, and measure of stability robustness are selected for control objective functions.[8] The state error energy and the control energy are defined as follows:

$$J_2 = \int_0^\infty \{x\}^T[Q_s]\{x\}\,\mathrm{d}t \tag{27}$$

$$J_3 = \int_0^\infty \{u\}^T[Q_u]\{u\}\,\mathrm{d}t \tag{28}$$

where the positive definite weighting matrices $[Q_s]$ and $[Q_u]$ should be selected to make the integrands correspond to physical energy measures. These objective functions are easily evaluated by solving the following Lyapunov matrix equations:

$$[P_s][A_c] + [A_c]^T[P_s] + [Q_s] = [0] \tag{29}$$

$$[P_u][A_c] + [A_c]^T[P_u] + [G]^T[Q_u][G] = [0] \tag{30}$$

Rewriting J_2 and J_3 in terms of $[P_s]$ and $[P_u]$,

$$J_2 = \mathrm{tr}([P_s][X_0]) \tag{31}$$

$$J_3 = \mathrm{tr}([P_u][X_0]) \tag{32}$$

where $[X_0]$ is a matrix defined by the outer product of initial condition, $[X_0] = \{x_0\}\{x_0\}^T$, and tr( ) is the trace of the matrix. Note that state error energy J_2 and control energy J_3 depend on initial states. $[X_0]$ can be chosen to represent some a priori statistical covariance of the distribution of initial conditions. We assume that the expected initial state is distributed over the unit sphere, and the identity matrix is taken for matrix $[X_0]$.

Because the sensitivity of the eigenvalues due to perturbations in the closed-loop system matrix depends on the condition number of the eigenvector matrix, the condition number of the eigenvector matrix is considered as a measure of stability robustness[23]:

$$J_4 = \|[\Phi_c]\|_2 \left\|[\Phi_c]^{-1}\right\|_2 = \frac{\sigma_1([\Phi_c])}{\sigma_n([\Phi_c])} \tag{33}$$

where σ_1 and σ_n denote the maximum and minimum singular values of the matrix $[\Phi_c]$, respectively, and $\|\ \|_2$ represents the Euclidean norm.

The electric power requirement for vibration suppression is also considered as the objective function. The electric power required for the control due to the harmonic disturbances is expressed as

$$\mathcal{P}(\omega)_{\mathrm{req}} = \sum_{i=1}^{m} |I_{0i}\,V_{ci}|_\omega \tag{34}$$

where V_{ci} denotes the applied control voltage to the ith PZT actuators due to the harmonic disturbance with initial magnitude $\{x_0\}$ and a specified frequency ω and, therefore,

$$\{V_c\} = -[G]\{x_0\} \tag{35}$$

The required total power is defined as the summation of the electric power with the assumption of harmonic disturbances with the frequency ranging from 1 to 200 Hz:

$$J_5 = \sum_{\omega=1}^{200} \mathcal{P}(\omega)_{\mathrm{req}} \tag{36}$$

The total number of structural/control design variables is 49. The x and y coordinates of the eight PZT actuators, pzx_i and pzy_i, are considered as the control design variables. The thickness distribution of the θ_i layer is expressed as the following cubic equation using thickness coefficients c^i_{jk}, and the ply orientation and the thickness coefficients of the composite layer are considered as the structural design variables:

$$t_i(x, y) = \sum_{j=0}^{3}\sum_{k=0}^{j} c^i_{jk} x^{j-k} y^k \tag{37}$$

The 60 constraints considered are as follows.

1) There are 30 constraints on minimum ply thickness (minimum strain gauge):

$$t_i(x_r, y_s) > 0, \qquad x_r = 0, 3, 6, \qquad y_s = 0, 6, 12 \tag{38}$$

2) The first three open-loop natural frequencies are considered as the constraints

$$\omega_i > \omega_{il}, \qquad i = 1, 2, 3 \tag{39}$$

where ω_{il} denotes the lower bounds for the ith mode's natural frequency ω_i.

3) There are 28 constraints on the placement of the eight piezoelectric actuators without overlapping:

$$|pzx_i - pzx_j| > 1.5 \quad \text{or} \quad |pzy_i - pzy_j| > 1.5$$
$$i = 1, \ldots, 8, \qquad j = i, \ldots, 8 \tag{40}$$

4) Constraints on static tip displacement as well as twist are considered to avoid too much flexibility to the structure.

There are also side constraints on the design variables for the actuators to be placed in the plate boundary. The numerical solution to the nonlinear optimization problem is obtained by using the sequential linear programming method with move limits in the general optimization program ADS.[24]

VI. Sensitivity Analysis

The information of the first-order derivatives is required in the optimization process for iterative direction search. The partial derivatives of the objective functions are evaluated by using the analytic formulation.

Sensitivity of the Objective Functions

The partial derivative of the weight of the composite plate is written as follows:

$$\Delta_i J_1 = \sum_{k=1}^{nop} \int_x \int_y \bar{\rho} \Delta_i t_k(x, y)\, \mathrm{d}x\, \mathrm{d}y \tag{41}$$

$\Delta_i(\,)$ denotes the partial derivatives of $(\,)$ with respect to the ith element of the design parameter. Note that the thickness distribution of the composite plate $t_k(x, y)$ is expressed as a simple function of x, y, and the thickness coefficient c_{ij} (structural design variables), as in Eq. (37).

The partial derivatives of the state error energy and control energy can be obtained as follows[8]:

$$\Delta_i J_2 = 2\,\mathrm{tr}\{[V][P_s][\Delta_i A_c]\} \tag{42}$$

$$\Delta_i J_3 = 2\,\mathrm{tr}\Big\{[V]\Big([P_u][\Delta_i A_c] + [G]^T[Q_u][\Delta_i G]\Big)\Big\} \tag{43}$$

where $[V]$ satisfies the complementary Lyapunov equation

$$[A_c][V] + [V][A_c]^T = -[X_0] \tag{44}$$

and

$$[\Delta_i A_c] = [\Delta_i A] - [\Delta_i B][G] - [B][\Delta_i G] \tag{45}$$

Robust measure's derivatives $\Delta_i J_4$ can be computed as follows[23]:

$$\Delta_i J_4 = \frac{(\Delta_i \sigma_1)\sigma_n - \sigma_1(\Delta_i \sigma_n)}{\sigma_n^2} \tag{46}$$

with

$$\Delta_i \sigma_j = \Re\Big(\{U\}_j^H [\Delta_i \Phi_c]\{V\}_j\Big) \tag{47}$$

where $\Re(\,)$ denotes the real part of the given value and $\{U\}_j$ and $\{V\}_j$ are the right and left unitary vectors computed by singular value decomposition of the closed-loop eigenvector matrix $[\Phi_c]$, where

$$[\Phi_c] = [U][\Sigma][V]^H \tag{48}$$

Note that the closed-loop eigenvector also depends on the control algorithm.

The partial derivative of the power requirement for vibration control can be obtained as follows:

$$\Delta_i J_5 = \sum \frac{1}{|S|}\{\Re(S)\Re(\Delta_i S) + \Im(S)\Im(\Delta_i S)\} \tag{49}$$

where

$$S(\omega) = \{I_0(\omega)\}^T[G]\{x_0\} \tag{50}$$

$$\Delta_i S = \{\Delta_i I_0\}^T[G]\{x_0\} + \{I_0\}^T[\Delta_i G]\{x_0\} \tag{51}$$

$$\{\Delta_i I_0\} = (j\omega/k_s)\Big\{[\Delta_i C_c][j\omega[I] - [A_c]]^{-1}[B][C] + [C_c]$$
$$\times \Big[\Delta_i (j\omega[I] - [A_c])^{-1}\Big][B][C] + [C_c]\Big[[j\omega[I] - [A_c]]^{-1}\Big]$$
$$\times [\Delta_i B][C] + [C_c]\Big[[j\omega[I] - [A_c]]^{-1}\Big][B][\Delta_i C]\Big\}\{x_0\} \tag{52}$$

with

$$[\Delta_i C_c] = [\Delta_i C] - [D][\Delta_i G] \tag{53}$$

$$\Big[\Delta_i (j\omega[I] - [A_c])^{-1}\Big] = [j\omega[I] - [A_c]]^{-1}[\Delta_i A_c]$$
$$\times [j\omega[I] - [A_c]]^{-1} \tag{54}$$

The sensitivity of the system matrices $[\Delta_i A]$, $[\Delta_i B]$, and $[\Delta_i C]$ is calculated by finite difference.

Sensitivity Analysis of the EAR

The sensitivity analysis for EAR has been performed analytically and is summarized as follows. First, the partial derivatives of the open-loop eigenvalue and eigenvector[23] and the closed-loop (desired) eigenvalues are derived as follows:

$$\Delta_i \lambda_j^o = \{\psi^o\}_j^T [\Delta_i A]\{\phi^o\}_j \tag{55}$$

$$\Delta_i \lambda_j^c = -\frac{\Im\big(\Delta_i \lambda_j^o\big)\zeta_j}{\sqrt{1 - \zeta_j^2}} + j\,\Im\big(\Delta_i \lambda_j^o\big) \tag{56}$$

$$\big\{\Delta_i \phi^o\big\}_j = \sum_{k=1}^{n} a_{jk}\{\phi^o\}_k \tag{57}$$

where the a_{jk} is given by

$$a_{jk} = \frac{1}{\lambda_j^o - \lambda_k^o}\{\psi^o\}_k^T[\Delta_i A]\{\phi^o\}_j, \qquad j \neq k$$
$$= -\sum_{\substack{l=1 \\ l \neq j}}^{n} a_{jl}\{\phi^o\}_l^T\{\phi^o\}_j, \qquad j = k \tag{58}$$

Note that $\{\phi^o\}_j$ and $\{\psi^o\}_j$ are the normalized open-loop right and left eigenvectors, respectively. Because the open-loop eigenvectors are used as the target eigenvector, $\{\Delta_i \phi^o\}_j$ represents the sensitivities of the target eigenvector.

From Eq. (16), the sensitivity of the parameter matrix $[\Delta_i H]$ can be expressed as

$$[\Delta_i H] = [B]^\dagger\{[\Delta_i A][\Phi_T] + [A][\Delta_i \Phi_T] - [\Delta_i \Phi_T][\Lambda_D]$$
$$- [\Phi_T][\Delta_i \Lambda_D]\} + [\Delta_i B]^\dagger([A][\Phi_T] - [\Phi_T][\Lambda_D]) \tag{59}$$

where $[\Delta_i \Phi_T]$ denotes the sensitivity of the target eigenvector and can be computed using Eqs. (57) and (58). The partial derivatives of the pseudoinverse $[\Delta_i B]^\dagger$ can be derived as follows:

$$[\Delta_i B]^\dagger = -\{[B]^T[B]\}^{-1}\Big\{[\Delta_i B]^T[B] + [B]^T[\Delta_i B]\Big\}$$
$$\times \{[B]^T[B]\}^{-1}[B]^T + \{[B]^T[B]\}^{-1}[\Delta_i B]^T \tag{60}$$

From Eq. (13), the partial derivative of the closed-loop eigenvector is obtained as follows:

$$\{\Delta_i \phi^c\}_j = \left([A] - \lambda_j^c[I]\right)^{-1}\left([\Delta_i B]\{h\}_j + [B]\{\Delta_i h\}_j + \Delta_i \lambda_j^c \{\phi^c\}_j - [\Delta_i A]\{\phi^c\}_j\right) \quad (61)$$

Finally, the partial derivative of the gain matrix is obtained from Eq. (17):

$$[\Delta_i G] = [\Delta_i H][\Phi_c]^{-1} - [H][\Phi_c]^{-1}[\Delta_i \Phi_c][\Phi_c]^{-1} \quad (62)$$

The partial derivatives of the closed-loop eigenvector $[\Delta_i \Phi_c]$ and gain matrix $[\Delta_i G]$ are used to compute the sensitivities of the objective functions.

VII. Numerical Example

A plate model containing eight sets of piezoelectric actuators is used as a model for the control system design. Each piezoactuator is 1.5×1.5 in. in size. The material properties used are given in Table 1 (Ref. 19). The laminate has six symmetric layers $[\theta_1/\theta_2/\theta_3]_s$. Initially, each layer has a uniform thickness of 0.03, 0.015, and 0.015 in., respectively. The initial ply orientations are $\theta_i = 0, +45, -45$, respectively. And the initial coordinates of the piezoactuators are presented in Table 2. The structural weight, control objective functions, and electric power for the initial geometry are $J_1 = 0.5$ lb, $J_2 = 7.60 \times 10^4$, $J_3 = 1.08 \times 10^{12}$, $J_4 = 1.02 \times 10^4$, and $J_5 = 7.46 \times 10^{-2}$, respectively. Weighting factors W_i in the objective functions are set to be 4, 4, 4, 4, and 1, respectively. These values are given arbitrarily. The reduction factor r_f is set as 0.5, and the initial move limit is set as 0.25. This move limit is reduced to ensure automatic convergence in the optimization tool as the optimization process continues. The constraints on natural frequencies are reasonably set to be $\omega_{il} = 10$, 30, and 70 Hz. The constraints on closed-loop damping ratios are taken as $\zeta_1 = 0.4$, $\zeta_2 = 0.25$, $\zeta_3 = 0.25$, $\zeta_4 = 0.18$, $\zeta_5 = 0.18$, and $\zeta_i = 0.1$ for the higher modes. The static tip displacement and twist are not allowed to be larger than 0.4 in. and 2.0 deg, respectively.

Figure 2 illustrates the iteration histories of the integrated structure/control objective function. The optimized values of the structural weight and control performance indices are $J_1 = 0.30$ lb, $J_2 = 5.04 \times 10^4$, $J_3 = 0.18 \times 10^{12}$, $J_4 = 0.53 \times 10^4$, and $J_5 = 3.31 \times 10^{-2}$, respectively. Figure 2 shows the reduction in the objective functions of 40, 34, 83, 48, and 56%, respectively. The objective function $\mathcal{J}$ converges to the final value of 0.807 from 2.236. The ply orientations of the laminated plate are changed from [0/45/−45] deg to [120.8/56.2/−41.1] deg. Natural frequencies ω_i for the initial model are $\omega_i = 17.5, 90.9$, and 104.1 Hz. And those values changed to 18.7, 73.7, and 119.6 Hz are all inactive. The tip displacement and twist are changed from 0.27 in. and 0.80 deg to 0.40 in. and 2.0 deg, respectively. The constraints on the tip displacement and twist are

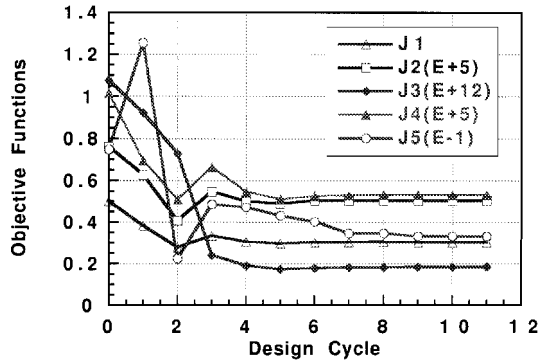

a) Structural/control objective functions

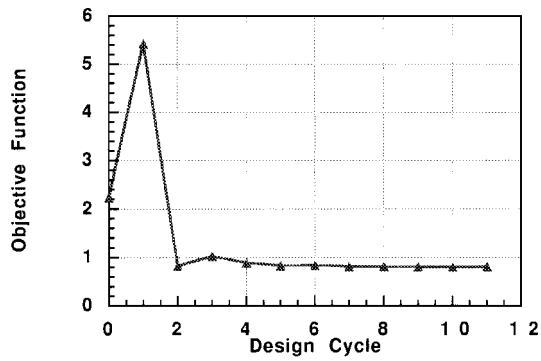

b) Total objective function

Fig. 2 Iteration histories of performance index.

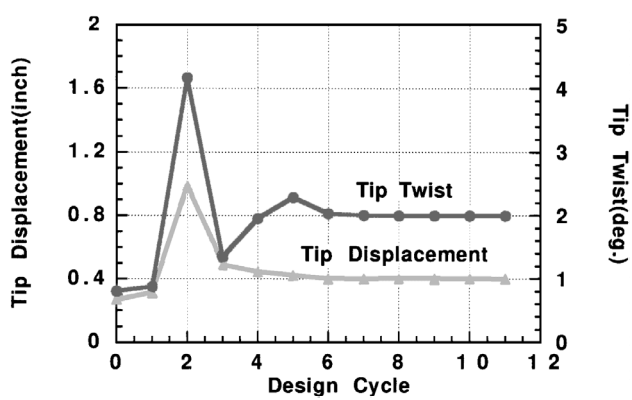

Fig. 3 Iteration histories of the tip constraints due to unit load.

Table 1 Material properties

Composite materials	Piezoelectric materials
$E_1 = 14.21 \times 10^6$ psi	$E_p = 9.137 \times 10^6$ psi
$E_2 = 1.146 \times 10^6$ psi	$\rho_p = 0.28$ lb/in.^{3}
$G_{12} = 0.8122 \times 10^6$ psi	$\nu_p = 0.3$
$\bar{\rho} = 0.05491$ lb/in.^{3}	$d_{31} = 6.5 \times 10^{-9}$ in./V
$\nu_{12} = 0.28$	$d_{32} = 6.5 \times 10^{-9}$ in./V

Table 2 Piezoelectric actuator locations

PZT number	Initial configuration	Optimized configuration
1	(0.50, 0.50)	(0.77, 0.53)
2	(0.50, 2.50)	(0.77, 2.13)
3	(0.50, 4.50)	(1.25, 4.73)
4	(0.50, 6.50)	(0.55, 8.90)
5	(3.50, 0.50)	(4.07, 0.09)
6	(3.50, 2.50)	(3.81, 1.94)
7	(3.50, 4.50)	(4.09, 3.46)
8	(3.50, 6.50)	(2.64, 7.13)

active (Fig. 3). Figure 4 shows the thickness distribution of the optimized configuration. It is thickest at the root and becomes thinner toward the tip. The optimized locations of piezoelectric actuators are shown in Fig. 5 and summarized in Table 2. As shown in Fig. 5, one actuator is placed at the tip and the leading-edge region. The other actuator sets are made to approach the root region to control the bending and twist motion more efficiently.

To compare the control performance of optimized configuration to that of initial model, the response and the control input histories are plotted. The closed-loop time histories of the tip displacement due to an initial disturbance are shown in Fig. 6. The corresponding control input voltages applied to PZT actuators for the control are shown in Figs. 7 and 8. The optimized model shows the faster response time, substantial reduction in vibration modes, and substantial decrease in control voltages applied to PZT actuators. Figure 8 shows that the optimized geometry is more efficient for vibration suppression. There are also substantial savings in the required electric power for vibration suppression of structure through the optimization process.

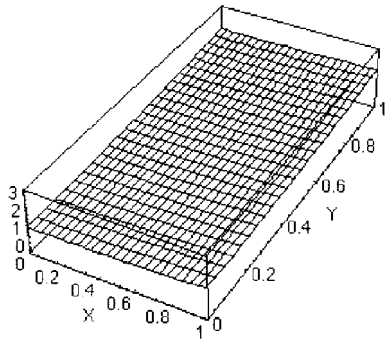

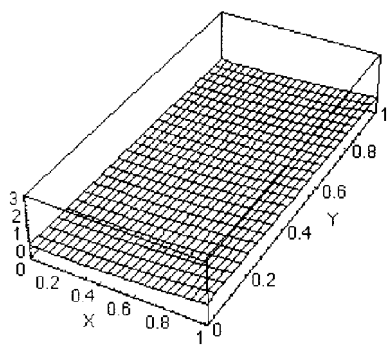

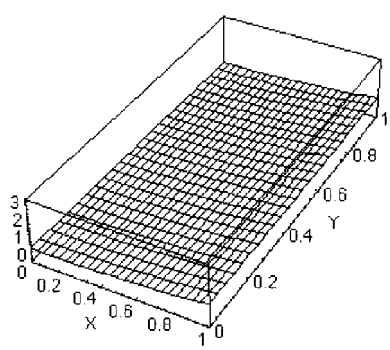

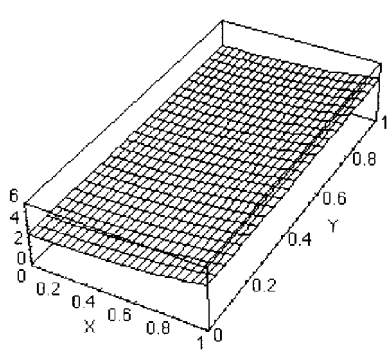

Fig. 4 Optimized thickness distribution of the composite layer (thickness $\times 10^{-2}$ in.).

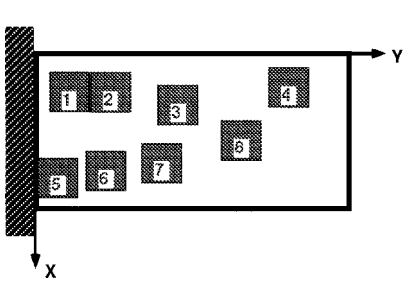

Fig. 5 Optimized locations of the PZT.

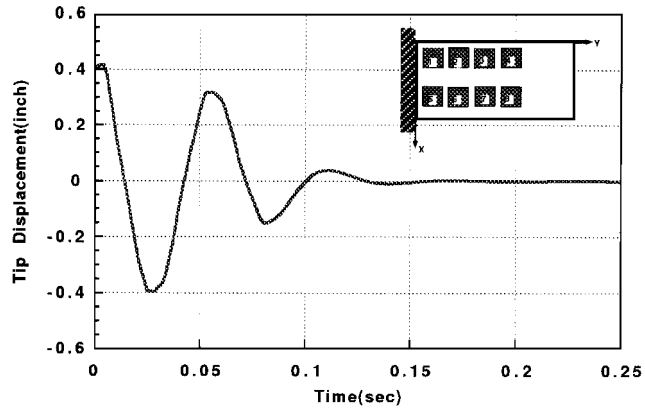

a) Initial configuration

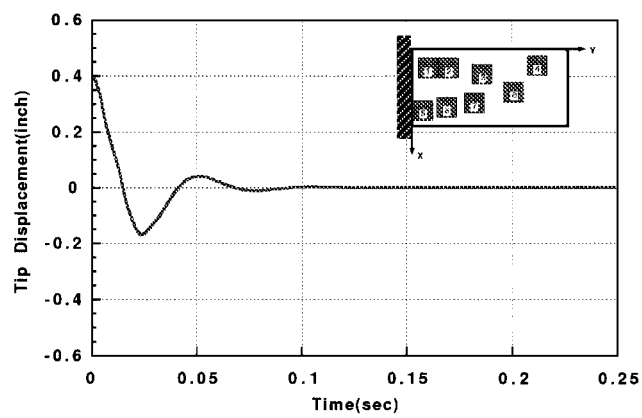

b) Optimized configuration

Fig. 6 Closed-loop responses.

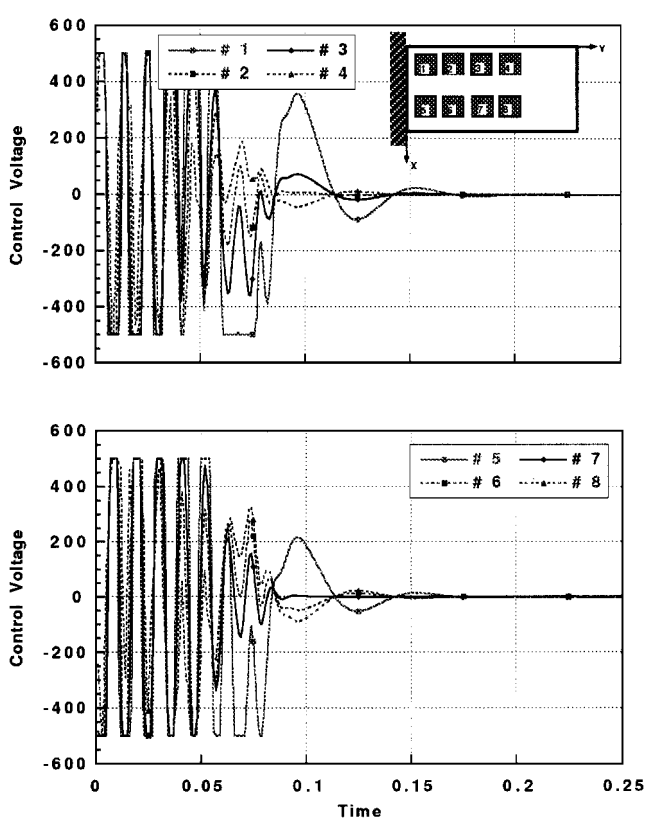

Fig. 7 Control voltages to the PZT actuators (initial configuration).

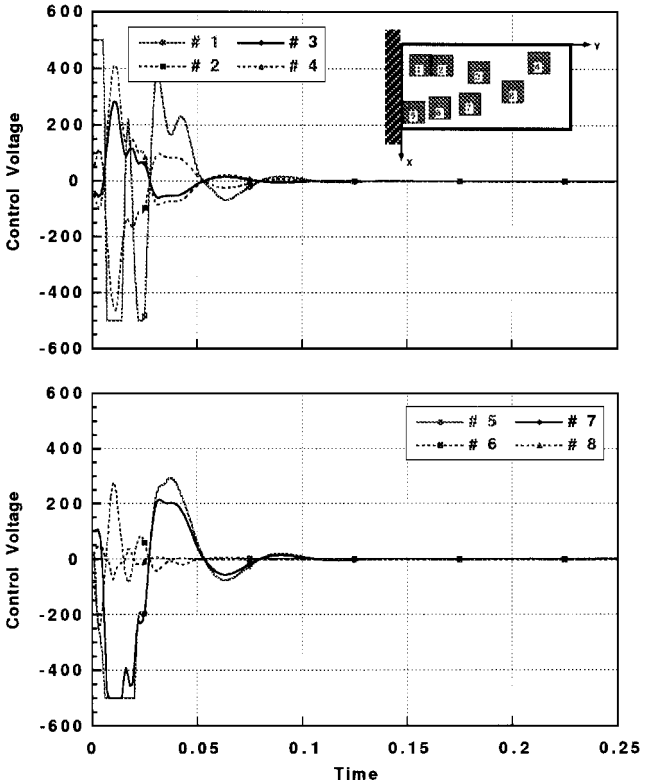

Fig. 8 Control voltages to the PZT actuators (optimized configuration).

VIII. Summary

The main objective is to propose a new simultaneous optimum design of the structure and control system for vibration suppression. To design the control system, a robust eigenstructure assignment scheme is adopted. The locations of the eight piezoelectric actuators are considered as the control design variables, and the ply orientation and the thickness coefficients of the composite layer are considered as the structural design variables. The method to predict the power required for the control is presented, and the power is used as a part of the objective functions. Constraints are imposed on the natural frequency, static tip displacement, and twist due to point loads. To perform an accurate and efficient optimization process, a sensitivity analysis has been conducted for the eigenstructure assignment control scheme and performance indices. The integrated structure/control design was formulated as a constrained multiobjective optimization problem and solved via sequential linear programming. The numerical results show that integrated optimum design of a structure and a control system not only improves performance but also reduces the cost of active control.

Acknowledgment

This work is supported by a research fund of the Korea Science and Engineering Foundation (Grant 961-1001-009-2).

References

[1]Kajiwara, I., Tsujioka, K., and Nagamatsu, A., "Approach for Simultaneous Optimization of a Structure and Control System," *AIAA Journal*, Vol. 32, No. 4, 1994, pp. 866–873.

[2]Nam, C., and Kim, Y., "Optimal Design of Composite Lifting Surface for Flutter Suppression with Piezoelectric Actuators," *AIAA Journal*, Vol. 33, No. 10, 1995, pp. 1897–1904.

[3]Sunar, M., and Rao, S. S., "Optimal Selection of Weighting Matrices in Integrated Design of Structures/Controls," *AIAA Journal*, Vol. 31, No. 4, 1993, pp. 714–720.

[4]Slater, G. L., and McLaren, M. D., "Disturbance Model for Control/Structure Optimization with Full State Feedback," *Journal of Guidance, Control, and Dynamics*, Vol. 16, No. 3, 1993, pp. 523–533.

[5]Suzuki, S., and Yonezawa, S., "Simultaneous Structure/Control Design Optimization of a Wing Structure with a Gust Load Alleviation System," *Journal of Aircraft*, Vol. 30, No. 2, 1993, pp. 268–274.

[6]Onoda, J., and Watanabe, N., "Integrated Direct Optimization of Structure/Regulator/Observer for Large Flexible Spacecraft," *AIAA Journal*, Vol. 28, No. 9, 1990, pp. 1677–1685.

[7]Nam, C., Kim, D., and Nam, S., "Integrated Structure/Control Design of Composite Plate with Piezoelectric Actuators," *Proceedings of the 19th Congress of the International Council of Aeronautical Sciences* (Anaheim, CA), AIAA, Washington, DC, 1994, pp. 604–611.

[8]Rew, D. W., and Junkins, J. L., "Multi-Criterion Approaches to Optimization of Linear Regulators," *Journal of the Astronautical Sciences*, Vol. 36, No. 3, 1988, pp. 199–217.

[9]Rao, S. S., Venkayya, V. B., and Khot, N. S., "Optimization of Actively Controlled Structures Using Goal Programming Techniques," *International Journal for Numerical Methods in Engineering*, Vol. 26, No. 1, 1988, pp. 183–197.

[10]Crawley, E. F., and Lazarus, K. B., "Induced Strain Actuation of Isotropic and Anisotropic Plates," *AIAA Journal*, Vol. 29, No. 6, 1991, pp. 944–951.

[11]Crawley, E. F., and Anderson, E. H., "Detailed Models of Piezoceramic Actuation of Beams," *Journal of Intelligent Material Systems and Structures*, Vol. 1, No. 1, 1990, pp. 4–25.

[12]Tzou, H. S., and Zhong, J. P., "Adaptive Piezoelectric Shell Structures; Theory and Experiments," *Proceedings of the AIAA 32nd Structures, Structural Dynamics, and Materials Conference* (Baltimore, MD), AIAA, Washington, DC, 1991, pp. 2290–2296 (AIAA Paper 91-1238).

[13]Lee, C. K., O'Sullivan, T. C., and Chiang, W. W., "Piezoelectric Strain Rate Sensor and Actuator Designs for Active Vibration Control," *Proceedings of the AIAA 32nd Structures, Structural Dynamics, and Materials Conference* (Baltimore, MD), AIAA, Washington, DC, 1991, pp. 2197–2208 (AIAA Paper 91-1064).

[14]Wang, B., and Rogers, C. A., "Modelling of Finite-Length Spatially-Distributed Induced Strain Actuators for Laminate Beams and Plates," *Proceedings of the AIAA 32nd Structures, Structural Dynamics, and Materials Conference* (Baltimore, MD), AIAA, Washington, DC, 1991, pp. 1511–1520 (AIAA Paper 91-1258).

[15]Preumont, A., Dufour, J., and Malekian, C., "Active Damping by a Local Force Feedback with Piezoelectric Actuators," *Journal of Guidance, Control, and Dynamics*, Vol. 15, No. 2, 1992, pp. 390–395.

[16]Hanagud, S., Obal, M. W., and Calise, A. J., "Optimal Vibration Control by the Use of Piezoceramic Sensors and Actuators," *Journal of Guidance, Control, and Dynamics*, Vol. 15, No. 5, 1992, pp. 1199–1206.

[17]Nam, C., Kim, Y., and Lee, K., "Optimal Wing Design for Flutter Suppression with PZT Actuators Including Power Requirement," *Proceedings of the AIAA/NASA/ISSMO 6th Symposium on Multidisciplinary Analysis and Optimization* (Bellevue, WA), AIAA, Reston, VA, 1996, pp. 36–46 (AIAA Paper 96-3984).

[18]Zhou, S., Liang, C., and Rogers, C. A., "Coupled Electro-Mechanical Impedance Modeling to Predict Power Requirement and Energy Efficiency of Piezoelectric Actuators Integrated with Plate-Like Structures," *Proceedings of the AIAA/ASME Adaptive Structures Forum* (Hilton Head, SC), AIAA, Washington, DC, 1994, pp. 259–269 (AIAA Paper 94-1762).

[19]Kim, Y., Kum, D., and Nam, C., "Simultaneous Optimization of Structural/Control Design Utilizing Eigenstructure Assignment Scheme," *Proceedings of the AIAA/NASA/ISSMO 6th Symposium on Multidisciplinary Analysis and Optimization* (Bellevue, WA), AIAA, Reston, VA, 1996, pp. 891–901 (AIAA Paper 96-4079).

[20]Nam, C., Oh, S., and Kim, W., "Active Flutter Suppression of Composite Plate with Piezoelectric Actuators," *Proceedings of the AIAA/ASME Adaptive Structures Forum* (Hilton Head, SC), AIAA, Washington, DC, 1994, pp. 127–134 (AIAA Paper 94-1745).

[21]Cavin, R. K., III, and Bhattacharyya, S. P., "Robust Well-Conditioned Eigenstructure Assignment via Sylvester's Equation," *Journal of Optimal Control Applications and Methods*, Vol. 4, No. 3, 1983, pp. 205–212.

[22]Rew, D. W., Junkins, J. L., and Juang, J. N., "Robust Eigenstructure Assignment by a Projection Method: Application Using Multiple Optimization Criteria," *Journal of Guidance, Control, and Dynamics*, Vol. 12, No. 3, 1989, pp. 396–403.

[23]Junkins, J. L., and Kim, Y., *Introduction to Dynamics and Control of Flexible Structures*, AIAA, Washington, DC, 1993, Chaps. 2, 5.

[24]Vanderplatts, G. N., "ADS—A Fortran Program for Automated Design Synthesis," Version 1.10, Engineering Design Optimization, Inc., Santa Barbara, CA, 1985, Chap. 2.